Applied Surface Science 378 (2016) 253–258

Contents lists available at ScienceDirect

Applied Surface Science

journal homepage: www.elsevier.com/locate/apsusc

Anisotropic behavior of layer-by-layer films using highly disordered copper hexacyanoferrate(II) nanoparticles

Rafael N. Soek, Ariane Schmidt, Herbert Winnischofer, Marcio Vidotti*

Grupo de Pesquisa em Macromoléculas e Interfaces—Department of Chemistry, Universidade Federal do Paraná, C.P. 19032, CEP 81531-980 Curitiba, Paraná, Brazil

ARTICLE INFO

Article history:
Received 27 January 2016
Received in revised form 23 March 2016
Accepted 26 March 2016
Available online 28 March 2016

Keywords:
Copper hexacyanoferrate nanoparticles
Structural defects
Layer-by-Layer
Anisotropic behavior
FTIR reflectance

ABSTRACT

Copper hexacyanoferrate(II) (Cu*hcf*(II)) nanoparticles (NPs) were synthesized by using a simple and straightforward methodology using aqueous solution without the need of any further passivating agent. The 15 nm NPs (obtained by TEM) were fully characterized by XRD, FTIR and Raman spectroscopy that revealed a high number of structural defects. These structural defects are responsible to produce a strong internal dipole moment. This leads to an anisotropic growth onto the electrode surface by using the layer-by-layer technique. Specular Reflectance FTIR corroborates with our assumption. The defects are also responsible for the high electroactivity of the Cu*hcf*(II)NPs modified electrodes in sodium based electrolytes. Our results contrast with others in which the authors attributed the cell distortion as the main phenomenon.

1. Introduction

Prussian Blue (PB) and its analogues are nanoporous inorganic materials with zeolitic structure and variable stoichiometry. Usually it presents the general formula $A_xM'_y[M''(CN)_6]\cdot zH_2O$, where A is an alkali countercation, M' and M'' are the transition metal ions and *x*, *y* and *z* are the stoichiometric coefficients. These self-assembled cyanide bridged compounds are an early example of metal-organic frameworks (MOFs) [1]. Firstly resolved by Kegin and Miles [2], the crystal structure of PB and its analogues have a face-centered cubic structure with variable degrees of disorder in the form of absent $[M(CN)_6]^{n-}$ species [3,4]. The distribution of the vacancies left by those missing units throughout the crystal can be either randomic $Fm\bar{3}m$, or non-randomic $Pm\bar{3}m$, depending on the synthetic procedure [5]. These vacancies allied to the zeolitic nature of the PB analogues enables the diffusion and storage of several species By this way, PB analogues are interesting systems for the construction of modified electrodes towards applications, such as batteries [6], hydrogen storage devices [5] and ion-selective systems [7].

The well-known lack of electroactivity of PB modified electrodes in large solvated cations (such as Na^+ and NH_4^+) based electrolytes has driven the development of analogues where Fe(III) is replaced by another transition metals, such as Ni(II), Cu(II), Co(II), etc. Amongst the PB analogues, copper hexacyanoferrate(II) (Cu*hcf*(II)) attracts special interest due to its potential application in energy storage systems [8], high power battery electrodes [6], stationary phase in chromatography [9], electrochromic devices [10], sensors [11] and biosensors [12–15]. The enhanced electrochemical properties of the PB analogues have been assigned to a structural distortion with increase in the cell parameters which promotes the ionic exchange during redox reactions. The LbL technique is a simple approach to obtain intelligent designed, multilayer, redox-active composite films with novel synergistic properties. [16] The assembly of such systems relies mostly on the electrostatic interaction between the compounds used to form each layer, nevertheless different factors proved to be also important for the stabilization of the assembled films, such as hydrogen bonding [17–19], van der Waals forces [20], layer interpenetration [21–23], temperature [23] and solution ionic strength. Several applications of LbL materials has been proposed, such as cell imaging [24], anti-wear coating [25], electrochromic devices [26], sensors [27] and biosensors [15]. As far as our knowledge a detailed study on the preferential orientation of the inorganic nanoparticles in the layered film has not been documented so far.

Regarding the nanoparticle synthesis, it is very important to develop a simple, versatile, straightforward and cheap method that can be scaled-up. Considering this, the sol-gel process [28], thermolysis methods [29–31], surfactant-free routs [32,33], solvent-free reactions [34,35] and sonochemical-assisted synthesis

* Corresponding author.
E-mail address: mvidotti@ufpr.br (M. Vidotti).

http://dx.doi.org/10.1016/j.apsusc.2016.03.199
0169-4332/

[10,15,36] have received great attention. Herein, we synthesized Cu*hcf*(II) nanoparticles by using a simple and easily converted to a large scale method, and performed a detailed characterization in order do deeply investigate the immobilization process by the Layer-by-Layer electrostatic assembly technique (LbL) and draw up another perspective on the electroactivity of the material.

2. Experimental

2.1. Materials

$CuCl_2{\cdot}2H_2O$ (Synth), $K_4[Fe(CN)_6]{\cdot}3H_2O$ (Synth), KCl (Sigma-Aldrich), anhydrous KBr (Sigma-Aldrich) and poly(diallyldimethylammonium chloride) PDDA (M_w = 200,000–350,000 g mol^{-1}; wt. 20% in water; Sigma-Aldrich) were used as received. Deionized water, obtained using a Millipore, Milli-Q water system (18.2 MΩ cm^{-1}) was used in all experiments.

2.2. Synthesis of the Cuhcf(II) NPs

The synthesis of the Cu*hcf*(II) NPs was adapted from the method used by DeLongchamp et al. [26,37]. Equal volumes of 2.0 mmol L^{-1} aqueous solutions of copper(II) chloride and potassium hexacyanoferrate(II) were mixed under vigorous stirring. After 10 min of reaction, the colloidal suspension was centrifuged under 13400 rpm in order to separate the Cu*hcf*(II) NPs. The solid was washed with deionized water and centrifuged again. UV–vis spectroscopy was used to estimate the Cu*hcf*(II) stoichiometry ($(K_{1,30}Cu_{1,35}[Fe(CN)_6]$). The dark-red solid was dried in desiccator under vacumm and anhydrous calcium chloride for 24 h. After that, the solid was pulverized in a mortar for the further experiments. No sedimentation was observed in the Cu*hcf*(II) NPs suspensions even after six months of storage. All experiments were performed in triplicate to assure both reliability and reproducibility.

2.3. Immobilization of the Cuhcf(II)NPs

The LbL films were obtained adapting a method described in reference [38]. The indium tin oxide (ITO; Delta Technologies; Sheet resistance ≤ 12 Ω cm^{-2}) electrode was dipped in a 1% wt PDDA solution for 5 min, followed by immersion in water for 1 min; after that, the electrode was immersed in a 1% wt colloidal Cu*hcf*(II) NPs suspension, kept for 5 min and dipped again in water for 1 min. The successive repetition of the steps was made to produce multilayer films. The films obtained by this procedure were named as ITO/(PDDA/Cu*hcf*(II))$_x$, where x is the number of depositions.

2.4. Transmission electron microscopy (TEM)

From the Cu*hcf*(II) NPs suspension, aliquots of 10 μL were transferred to a FORMVAR™/Carbon covered 400 mesh copper grid (Ted Pella, Inc.) for TEM analysis. The samples were dried under vacuum overnight before the measurements. Jeol JEM 1200EXII Electron Microscope operating at 120 keV was used to obtain the Cu*hcf*(II) NPs images. Different regions of the grid from at least three different syntheses samples were analyzed. The software ImageJ ver. 1.48 was used for analysis.

2.5. Zeta (ζ-)Potential

Zetasizer Nano ZS90 was used for the ζ-Potential experiments of the Cu*hcf*(II)NPs suspension, using an Electrophoretic Light Scattering with a resolution of 0.12 μm cm V^{-1} s^{-1}. He-Ne (632.8 nm) laser was used as light source, with a maximum of 4.0 mW.

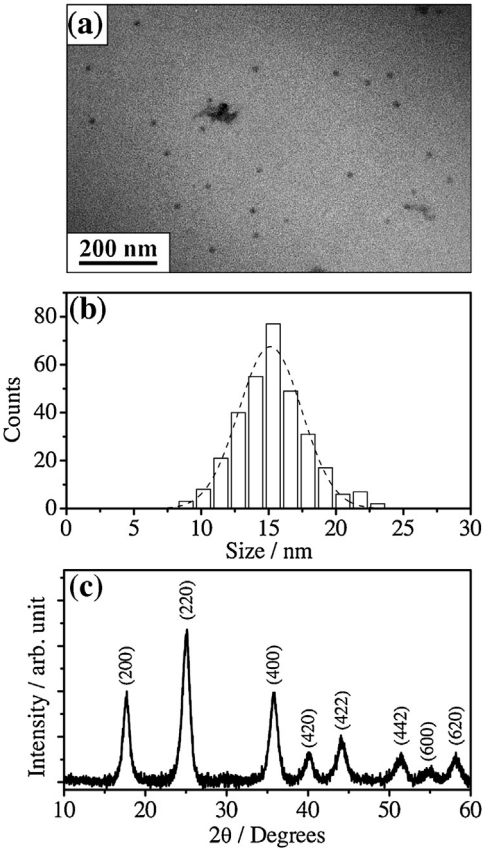

Fig. 1. (a) TEM image of Cu*hcf*(II) NPs of approximately 15 nm. (b) Histogram showing the size distribution of a population of 320 particles. (c) X-ray diffraction pattern of the Cu*hcf*(II) NPs corresponding to the $Fm\bar{3}m$ space group.

2.6. Vibrational Spectroscopy (FTIR and Raman)

The Bomem, Hartmann & Braun MB-Serie was used for FTIR experiments, in the 4000–400 cm^{-1} range, with 4 cm^{-1} resolution of the materials embedded in anhydrous KBr pellets. The Bruker Vertex 70 Spectrometer was used for Specular Reflectance FTIR experiments of the ITO/(PDDA/Cu*hcf*(II))$_x$ films using the A518/Q horizontal reflection unit 80° accessory, with 2 cm^{-1} nominal resolution. Raman measurements were made in a Renishaw Spectrophotometer using He-Ne laser (λ_o = 632.8 nm).

2.7. X-ray powder diffraction (XRD)

The Shimadzu LabX XRD-6000 was used, with a 0.02° nominal resolution, ranging from 10 to 60°, using glass holder, 3.0 s step time, 40.0 V and 30.0 A.

2.8. Electrochemistry

The Autolab PGSTAT-30 potentiostat/galvanostat was used for cyclic voltammetry of the *LbL* modified electrodes, using a three electrode cell with platinum and Ag/AgCl/Cl^-_{sat} as counter and reference electrodes, respectively. Aqueous KCl and NaCl (0.1 mol L^{-1}) were used as electrolyte solutions.

3. Results and discussion

The reddish color acquired by the suspension after mixing the precursors reveals the formation of the colloidal Cu*hcf*(II) NPs, as reported previously [10,15]. Fig. 1(a) shows a micrograph of the